Available online at www.sciencedirect.com
ScienceDirect
Ceramics International 37 (2011) 599–606
CERAMICS INTERNATIONAL
www.elsevier.com/locate/ceramint

Effects of bismuth oxide on the sinterability of hydroxyapatite

S. Ramesh [a,*], C.Y. Tan [a], W.H. Yeo [a], R. Tolouei [a], M. Amiriyan [a], I. Sopyan [b], W.D. Teng [c]

[a] Ceramics Technology Laboratory, COE, University Tenaga Nasional, Jalan IKRAM-UNITEN, 43009 Kajang, Selangor, Malaysia
[b] Department of Manufacturing and Materials Engineering, Faculty of Engineering, International Islamic University Malaysia, Malaysia
[c] Ceramics Technology Group, SIRIM Berhad, 1 Persiaran Dato Menteri, Shah Alam, Malaysia

Received 14 September 2009; received in revised form 9 September 2010; accepted 27 September 2010
Available online 28 October 2010

Abstract

The sinterability of Bi_2O_3-doped hydroxyapatite (HA) has been studied and compared with the undoped HA. Varying amounts of Bi_2O_3 ranging from 0.05 wt% to 1.0 wt% were mixed with the HA. The study revealed that most sintered samples composed of the HA phase except for compacts containing 0.3, 0.5 and 1.0 wt% Bi_2O_3 and when sintered above 1100 °C, 1000 °C and 950 °C, respectively. In general, the addition of 0.5 wt% Bi_2O_3 was identified as the optimum amount to promote densification as well as to improve the mechanical properties of sintered HA at low temperature of 1000 °C. Throughout the sintering regime, the highest value of relative bulk density of 98.7% was obtained for 0.5 wt% Bi_2O_3-doped HA when sintered at 1000 °C. A maximum Young's modulus of 119.2 GPa was measured for 0.1 wt% Bi_2O_3-doped HA when sintered at 1150 °C. Additionally, the ceramic was able to achieve highest hardness of 6.08 GPa and fracture toughness of 1.21 MPa $m^{1/2}$ at sintering temperature of 1000 °C.

Keywords: Hydroxyapatite; Bismuth oxide; Relative density; Young's modulus; Vickers hardness; Fracture toughness

1. Introduction

Hydroxyapatite (HA), $Ca_{10}(PO_4)_6(OH)_2$, is thermodynamically most stable calcium phosphate ceramic compound at the pH, temperature and composition of the physiological fluid [1]. It possesses similar chemical composition and crystallographic properties with the mineralized human bone [2]. Due to these reasons, synthetic HA exhibits strong affinity to host hard tissues. The current development of HA in medical application, however, is limited to only non-stressed application such as bone filler or coatings for metallic and bioinert implant. This limitation is mainly due to its low mechanical properties [3]. Consequently, a great number of studies have been devoted to overcome this limitation of HA [4–6].

Many studies have revealed that various properties of HA ceramics could be improved by using sintering additives. For instance, Fanovich and Lopez [7] found that addition of Mg^{2+} played a significant role in inhibiting grain growth of HA. Ramesh et al. [8] reported that small addition of MnO_2 in HA was beneficial in enhancing low temperature densification and mechanical properties such as hardness, fracture toughness and Young's modulus. In addition, the use of sintering additive has been reported as an economical method and effective sintering aids in order to improve the sinterability of HA [5].

Bismuth compounds have been used in clinical application. Today, the two major medicinal use of bismuth compound is focused on antimicrobial agent and anticancer agent [9]. Furthermore, recent research by Webster et al. [10] reported that among various dopants (Mg^{2+}, Zn^{2+}, La^{3+}, Y^{3+} and In^{3+}), Bi^{3+} was the most effective dopant in promoting osteoblast response to HA in human body. The authors also encourage researchers to further investigate the other effects of Bi_2O_3-doped HA in particular its sinterability, in order to determine its efficacy as an orthopedic/dental material [10]. Therefore, the primary objective of the current work was to study the sinterability of synthesized HA when doped with up to 1 wt% of bismuth oxide.

* Corresponding author. Current address: University of Malaya, Faculty of Engineering, 50603 Kuala Lumpur, Malaysia.
Tel.: +60 3 8928 7282; fax: +60 3 89212111.
E-mail address: ramesh@uniten.edu.my (S. Ramesh).

0272-8842/$36.00
doi:10.1016/j.ceramint.2010.09.041

2. Experimental procedure

2.1. Powder synthesis and sample preparation

The starting hydroxyapatite used in this work was prepared via a novel wet chemical precipitation method using precursors of $Ca(OH)_2$ and H_3PO_4. The detail procedures to synthesize the HA powder is described elsewhere [11]. The dopant used in this work was obtained from a commercial available Bi_2O_3 powder (Nanostructured & Amorphous Inc. USA; 99.9% purity having an average particle size of 150 nm) and amount of dopant used were 0.05, 0.1, 0.3, 0.5 and 1.0 wt%. For each composition, a 100 g batch of dry powder mixture, comprising the HA and Bi_2O_3, were mixed in 150 ml of ethanol and followed by ball milling for 1 h. In a typical mixture, the ball to powder ratio was kept at 1.5.

Table 1
Properties of the starting HA powders.

Calcium (as Ca), % (w/w)	38.9
Phosphorous (as P), % (w/w)	23.2
Ca/P ratio	1.677
Particle size (nm)	150 ± 50
Colour	White

After the mixing, the wet slurry was dried, crushed and sieved into powder form. Then, the obtained powder was

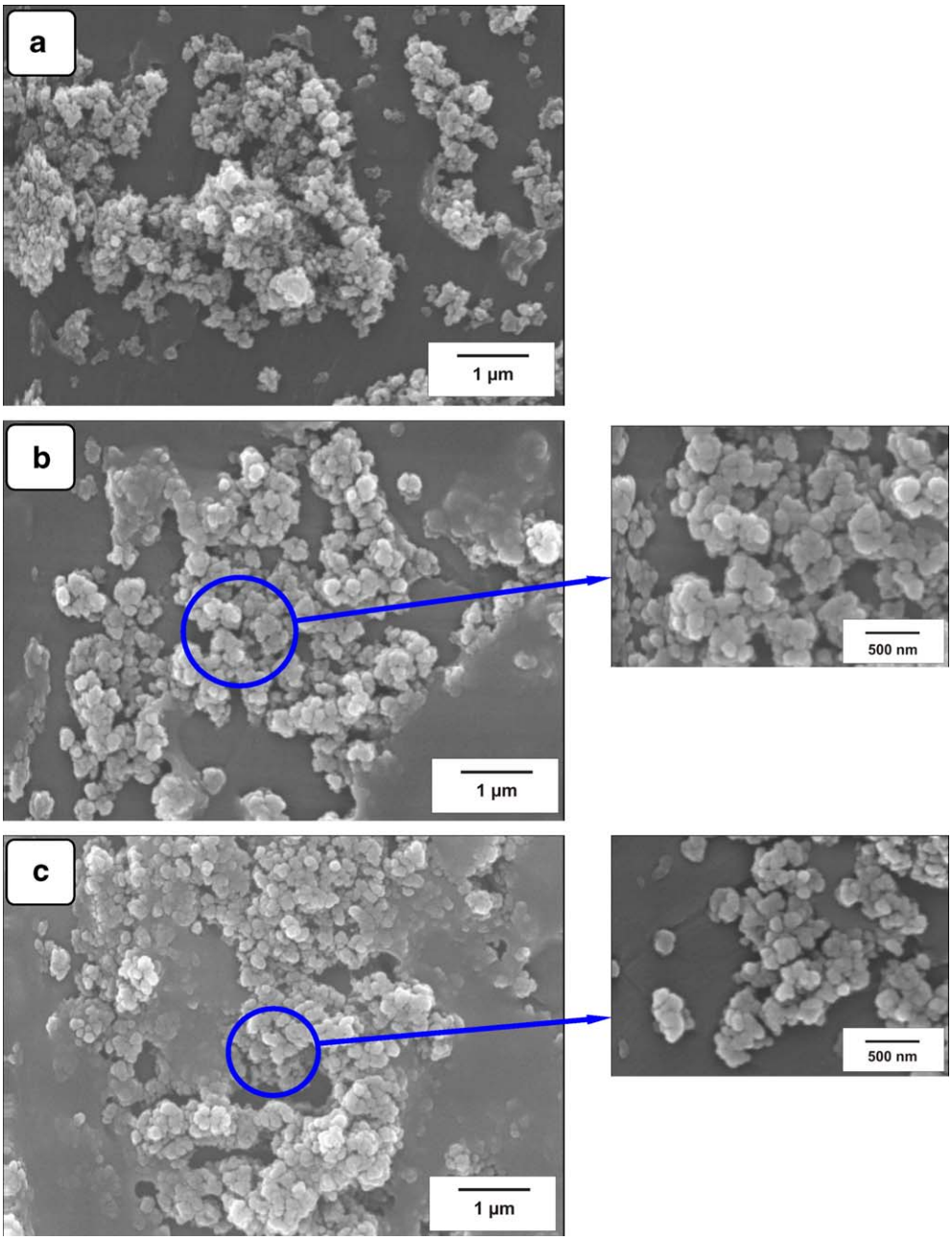

Fig. 1. SEM micrographs of powder particles. (a) Synthesized HA; (b) 0.5 wt% Bi_2O_3-doped HA; (c) 1.0 wt% Bi_2O_3-doped HA.

uniaxial pressed at 1.5–2.0 MPa into circular discs (20 mm diameter) and rectangular bars (4 mm × 13 mm × 32 mm) and subsequently cold isostatic pressed at 200 MPa (Riken Seiki, Japan).

2.2. Sintering and body characterisation

The compacted green samples were sintered at temperature ranging from 1000 to 1400 °C, with ramp rate of 2 °C/min and soaking time of 2 h. Prior to testing, all sintered samples were polished to 1 μm surface finish.

The calcium (Ca) and phosphorus (P) content in the synthesized HA powders were determined by using the Inductively Coupled Plasma-Atomic Emission Spectrometry (ICP-AES) technique. The particle size distributions of the HA powders was determined using a standard Micromeritics® SediGraph 5100 X-ray particle size analyzer. The phase stability studies of powders and sintered samples were carried out by using X-ray diffraction (XRD) (Geiger-Flex, Rigaku Japan). The bulk densities were obtained by water immersion technique (Mettler Toledo, Switzerland). The Young's modulus by sonic resonance was determined on rectangular samples using a commercial testing instrument (GrindoSonic: MK5 "Industrial", Belgium) [12]. The microhardness (H_v) and fracture toughness (K_{Ic}) of the samples were determined using the Vickers indentation method (Matsuzawa, Japan). The K_{Ic} value was calculated using the equation derived by Niihara [13]. The microstructural examination was conducted by using the scanning electron microscope (SEM).

3. Results and discussion

3.1. Powder properties

The results of the chemical analysis as well as the particle size of the derived HA powders are shown in Table 1.

The average particle size of the HA was small regardless of bismuth addition and this is evident from the SEM micrograph of the powders as shown in Fig. 1. However, the introduction of Bi_2O_3 in the HA powder was observed to have a distinct colour change, i.e. from white (undoped HA) to yellow (Bi_2O_3-doped HA). This colour change was more pronounced for powders which consisted of ≥0.3 wt% of Bi_2O_3. However, after sintering in air above 1000 °C, all samples were observed to be white in colour. Since the melting temperature of Bi_2O_3 is reported to be ~824 °C [14], it is believed that the Bi_2O_3 added could either be taken into solid solution with HA, with small portions of the melted Bi_2O_3 vaporized during sintering as suggested by Chiang et al. [15], Metz et al. [16] and Peiteado et al. [14].

3.2. X-ray diffraction

X-ray diffraction (XRD) analysis of the synthesized HA powder produced only peaks which corresponded to the standard JCPDS card no.: 74-0566 for stoichiometric HA as shown in Fig. 2. In addition, the XRD pattern of the synthesized powder was in good agreement with that of enamel of a human tooth. Thus, it is evident that the synthesized crystals were mainly single-phase HA and is believed to be very small as indicated by the peak broadening of the diffraction patterns [17]. Similar peak broadening of HA fine powders were reported by Liu et al. [18]. In general, no other secondary phases such as tricalcium phosphate (TCP), tetracalcium phosphate (TTCP) or calcium oxide (CaO) were detected in the all powders.

The XRD results of sintered samples indicated that most samples corresponded to HA phase except for compacts that contained 0.3, 0.5 and 1.0 wt% Bi_2O_3 sintered above 1100 °C, 1000 °C and 950 °C, respectively. This observation is not in agreement with earlier work reported by Webster et al. [10] who found that no decomposition was detected even for 5 wt% Bi_2O_3-doped HA when sintered at 1100 °C. However, the present research revealed that the HA phase was disrupted when 0.3 wt% Bi_2O_3 were added into HA and sintered above 1100 °C as shown in Fig. 3. Similar phase decomposition was also detected for 0.5 wt% Bi_2O_3-doped HA when sintered above 1000 °C. In the case of 1.0 wt% Bi_2O_3-doped HA, α-TCP was detected when sintered at 1000 °C.

In general, sintering of HA can lead to the partial thermal decomposition of HA into tricalcium phosphate (TCP) and/or tetracalcium phosphate (TTCP). The thermal decomposition is accompanied in two steps i.e. dehydroxylation and decomposition. Dehydroxylation to oxyhydroxyapatite proceeds at

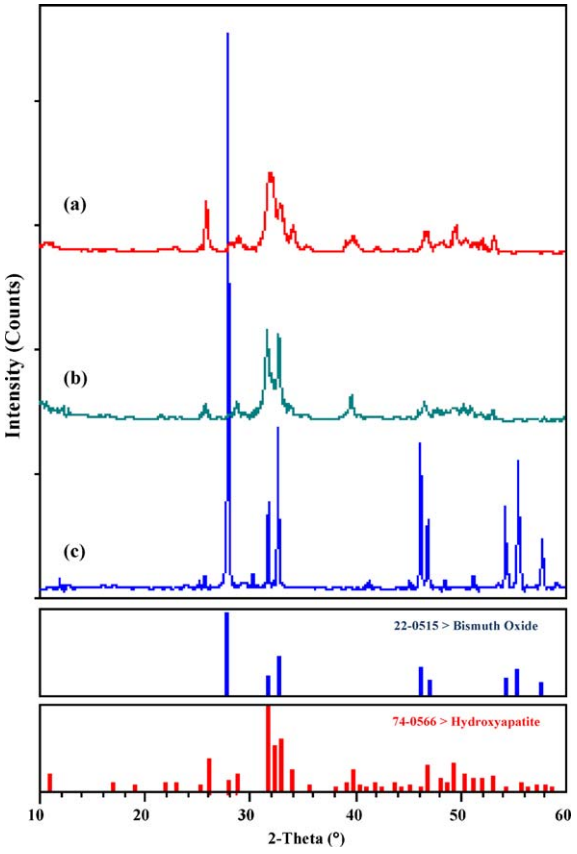

Fig. 2. Comparison of XRD patterns of (a) synthesized HA powder; (b) enamel of human tooth; (c) as-received bismuth powder.

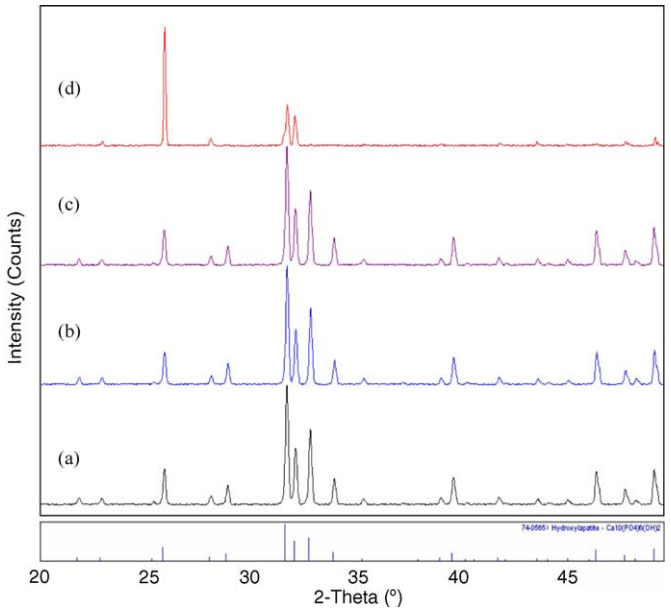

Fig. 3. XRD patterns of 0.3 wt% Bi_2O_3-doped HA samples sintered at (a) 1000 °C; (b) 1050 °C; (c) 1100 °C and (d) 1150 °C. Severe disruption of HA phase is evident in (d).

temperatures about 850–900 °C by the fully reversible reaction in accordance to equation 1 [19]:

$$Ca_{10}(PO_4)_6(OH)_2 \rightarrow Ca_{10}(PO_4)_6(OH)_{2-2x}O_x + xH_2O_{gas} \quad (1)$$

The decomposition to TCP and TTCP occur at temperatures greater than 900 °C according to the reaction given in Eq. (2) [20]:

$$Ca_{10}(PO_4)_6(OH)_2 \rightarrow 2Ca_3(PO_4)_2 + Ca_4P_2O_9 + H_2O_{gas} \quad (2)$$

According to the equations, both the dehydroxylation and decomposition reactions include water vapour as a product, the rates at which these reactions proceed depend on the partial pressure of H_2O in the furnace atmosphere. Thus, the secondary phase formation during sintering could be controlled by simply controlling the sintering atmosphere. The high humidity content present in the sintering atmosphere has the tendency to slow down the decomposition rate by preventing the dehydration of the OH group from the HA matrix. This can be achieved by controlling the partial pressure of the atmosphere, as the saturated moisture content in the atmosphere would suppress the by-product of water vapour between the reactions of both the dehydroxylation and decomposition [19].

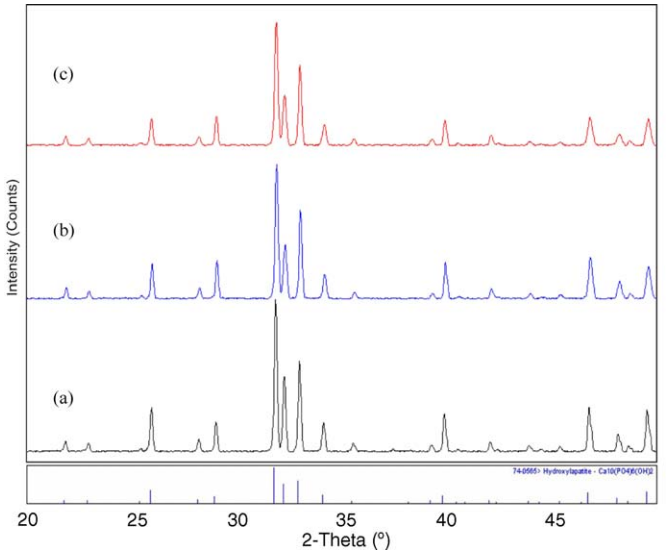

Fig. 4. XRD patterns of HA samples sintered at 1400 °C. (a) Undoped HA; (b) 0.05 wt%; (c) 0.1 wt% Bi_2O_3-doped HA. All peaks belong to HA phase.

However, from the XRD analysis, it shows that the contribution factor to the decomposition of HA was not due to dehydroxylation which was proposed by Wang et al. [19]. This is evident in Fig. 4 which shows that no TCP, TTCP or CaO was observed in undoped, 0.05 wt% and 0.1 wt% Bi_2O_3-doped HA even when sintered at 1400 °C in air. In the present work, excessive doping (0.3 wt% Bi_2O_3 and above) was the primary factor causing disruption of HA phase as typically shown in Fig. 3(d).

3.3. Relative density

The effect of Bi_2O_3 doping on the relative density of HA is shown in Fig. 5. The results indicated that the HA having high content of Bi_2O_3 (>0.3 wt%) exhibited higher densification, in particular at low sintering temperatures. For example, when sintered at 1000 °C, 0.5 wt% Bi_2O_3-doped HA achieved the highest relative density of 98.7% whereas undoped HA could only exhibit relative density of 95.5% when sintered at similar temperature. To further study the microstructure evolution of both samples, the SEM images in Fig. 7(a) revealed that undoped sample was porous and individual grain could still be observed at sintering temperature of 1000 °C. In contrast, no pores were observed in the 0.5 wt% Bi_2O_3-doped HA sample and compacted grain was clearly seen in Fig. 7(b) when sintered at 1000 °C. The remarkable achievement of 0.5 wt% Bi_2O_3-doped HA at 1000 °C has prompted further study on the densification at lower temperature such as 950 °C. However, in this attempt, the result showed that the relative density of the sintered HA body was low, at ~90%.

As for high sintering temperatures, higher content of bismuth proved to be detrimental to the densification of HA. This was evident since the 1.0 wt% Bi_2O_3-doped HA could only achieve relative density of approximately 96.1% as compared to 98.3% for undoped HA when sintered at 1400 °C. The deterioration of the densification in these samples could be attributed to the decomposition of HA phase as mentioned earlier. This is in agreement with observation reported by Suchanek et al. [4], Fanovich and Lopez [7] and Raynaud et al. [21] who revealed that decomposition of HA phase could eventually deteriorate the bulk density and mechanical properties of sintered HA body.

Throughout the sintering regime studied, the highest relative density of 98.7% was achieved when 0.5 wt% Bi_2O_3 was doped and sintered at 1000 °C. The beneficial effect of Bi_2O_3 in enhancing densification of HA could be attributed to the low melting point of dopant and subsequently resulted in liquid

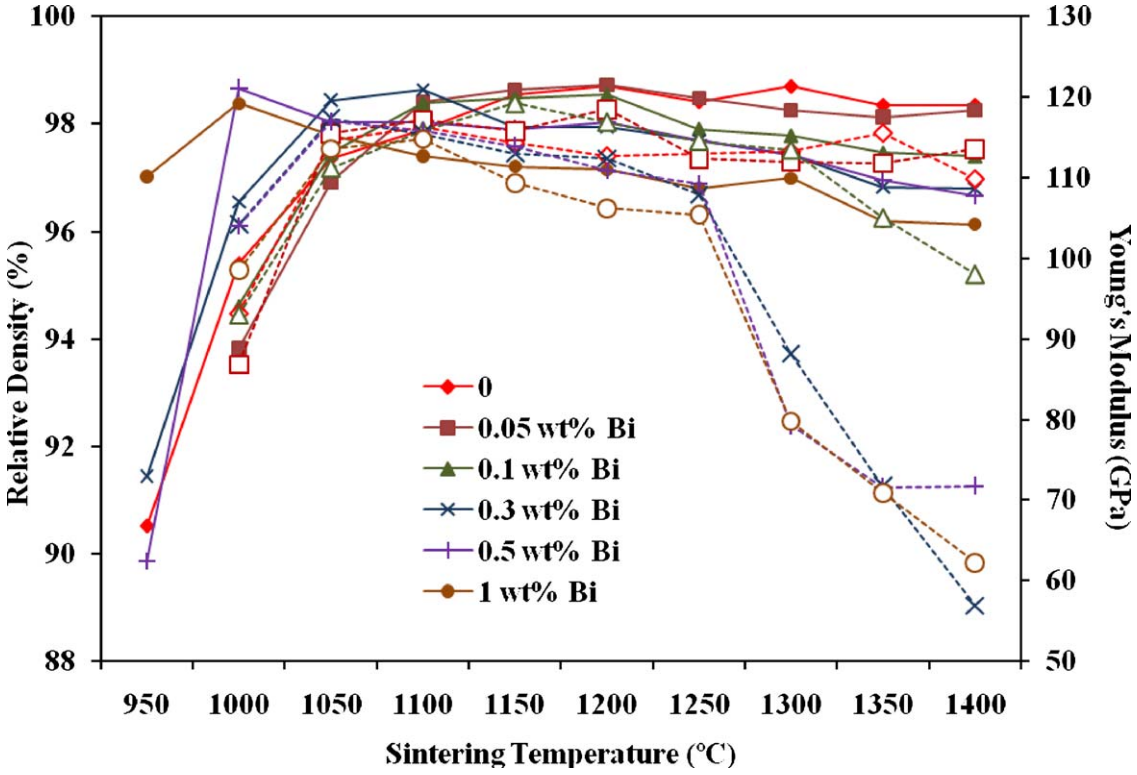

Fig. 5. Relative density (represented by full symbol and continuous line) and Young's modulus (represented by the open symbols and dotted line) variation as a function of dopant addition and sintering temperature.

phase sintering. Successful examples of using other low melting point additive as a sintering aid in HA have been discussed the literatures [4,6,22,23].

In the case of Bi_2O_3, its beneficial effect in aiding densification was reported in various ceramics system such as by Gil et al. [24], Yu et al. [25], Peiteado et al. [14] and Hirano et al. [26]. Gil et al. [24] who studied the densification process and microstructure development in Bi_2O_3-doped gadolinia ceria (GDC) ceramics, found that densification of GDC was strongly enhanced by adding small amounts of Bi_2O_3. For example, samples of GDC containing $\leq$1 wt% Bi_2O_3 sintered at 1200–1400 °C for 2–4 h achieved near theoretical density when compared to the undoped ceramic. The authors attributed this rapid densification to the low melting point of Bi_2O_3 (820 °C) which resulted in transient liquid phase-assisted sintering. When >1.0 wt% Bi_2O_3 was used, a decreased in density was observed at sintering temperature of 1350 °C. The authors inferred that this was due to both rapid volatilization of Bi_2O_3 and evolution of oxygen gas produced as consequence of some reduction of Ce^{4+} to Ce^{3+}. For the microstructure evolution, the authors found that Bi_2O_3 has no significant effect on the grain size of GDC ceramics body. On the other hand, Yu et al. [25] discovered the optimum addition of Bi_2O_3 (0.06 wt%) in MnZn ferrites has promoted the sintering process and grain growth, thus reduced porosity and enhance densification. When Bi_2O_3 content exceeded 0.06 wt%, the excessive liquid phase quickened the sintering process and the grain growth accelerated too fast for the pores to escape from inner grains. As a result, there were many abnormal large grains which have pores in them. Hirano et al. [26] studied the effect of Bi_2O_3 on the 10 mol% Sc_2O_3-stabilized zirconia (ScSZ). In this experiment, the authors found that ScSZ with additional 1 mol% Bi_2O_3 yielded dense sintered body at temperature of 1000 °C as compared to 1300 °C for undoped ScSZ. Based on the literature findings and the low melting point of Bi_2O_3, it is believed that a transient liquid phase could be responsible for the improved densification of HA at low sintering temperature.

3.4. Young's modulus, Vickers hardness and fracture toughness

The effect of Bi_2O_3 doping on the Young's modulus (E) of HA is shown along side with relative density in Fig. 5. The inclusion of Bi_2O_3 in HA, particularly for the higher dopant concentration, was found to be beneficial in enhancing the stiffness of the sintered HA body when sintered at low temperatures as depicted by the higher Young's modulus attained in these samples. Fig. 5 shows that the highest value of ~107 GPa was recorded for HA samples containing 0.5 wt% Bi_2O_3 when sintered at 1000 °C as compared to 93 GPa for undoped HA when sintered at similar temperature. However, when sintered above 1100 °C, the Young's modulus of 0.5 wt% Bi_2O_3-doped HA started to decrease to below that of the undoped HA.

In contrast, the undoped HA started at low E value (93 GPa) when sintered at 1000 °C and increased gradually to reach a plateau at temperature 1100 °C. Similarly, both the additions of

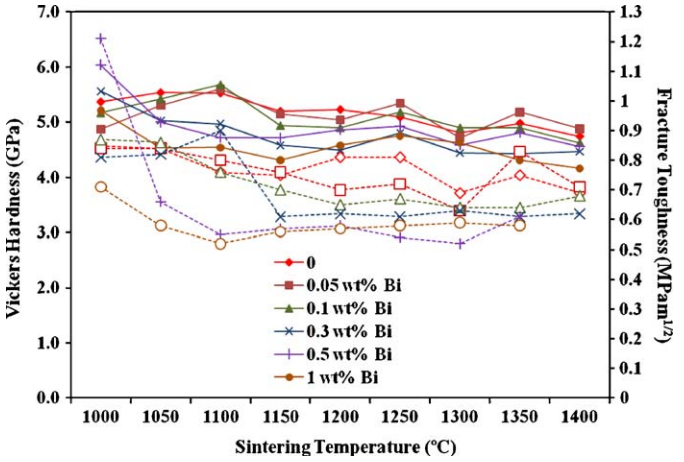

Fig. 6. The effect of bismuth oxide on the Vickers hardness (represented by full symbol and continuous line) and fracture toughness (represented by the open symbols and dotted line) of sintered HA.

0.05 wt% and 0.1 wt% exhibited the highest Young's modulus of ~119 GPa when sintered at 1100–1200 °C. Thereafter, the stiffness of the sintered body fluctuated slightly with increasing temperature. Throughout the sintering regime studied, the highest stiffness value of 119.2 GPa was obtained for 0.1 wt% Bi_2O_3-doped HA and when sintered at 1150 °C.

The effect of Bi_2O_3 and sintering temperature on the Vickers hardness of HA is shown in Fig. 6. In general, it can be noted from the graph that the Vickers hardness of HA with different additions of Bi_2O_3 varied in a similar manner as for relative density variation with sintering temperature. The results obtained in present work confirmed that both 0.3 wt% and 0.5 wt% Bi_2O_3-doped HA was beneficial in improving the hardness of HA when sintered at low temperature. However, when sintering temperature increased to 1050 °C, the hardness dropped drastically to ~5 GPa and further declined as the sintering temperature increased. In addition, as the dopant content increased to 1.0 wt%, the hardness value was found to decrease from 5.2 GPa to 4.5 GPa when sintered above 1050 °C.

In contrast, the hardness of undoped HA started at 5.4 GPa at 1000 °C and increased slightly to ~5.5 GPa at 1050–1100 °C. Subsequently, a decreasing trend was observed as the sintering temperature was increased. Similarly, the hardness of 0.05 wt% and 0.1 wt% Bi_2O_3-doped HA started low (4.9–5.2 GPa) at 1000 °C, and increased to the maximum to ~5.6 GPa at 1100 °C. Thereafter, the hardness decreased and fluctuated slightly as the sintering temperature was increased >1000 °C.

In comparison with other dopants reported in the literatures, bismuth was found to be beneficial in enhancing the Vickers hardness of sintered HA body at low temperature. For instance, Bandyopadhyay et al. [23] obtained maximum hardness of 4.8 GPa for 2.5 wt% ZnO-doped HA sintered at temperature of 1250 °C. Kalita et al. [27] revealed that maximum hardness of 4.6 GPa was attained when 2.5 wt% of 30% CaO + 30% P_2O_5 + 40% Na_2O glass system was used in HA and sintered at 1300 °C for 3 h. Filho et al. [28] attained highest hardness value of 5.7 GPa for 0.5 wt% Fe_2O_3-doped HA sintered at temperature of 1300 °C. However, in the present work, the advantage of using 0.5 wt% Bi_2O_3 was that the maximum hardness of 6.1 GPa was achieved at a much lower sintering temperature of 1000 °C. This excellent result in the improvement of Vickers hardness of Bi_2O_3-doped HA at low sintering temperature is associated with the improved densification as depicted in Fig. 5.

Similar to the Vickers hardness trend, the 0.5 wt% Bi_2O_3-doped HA achieved higher fracture toughness of 1.21 MPa $m^{1/2}$ as compared to 0.85 MPa $m^{1/2}$ for undoped HA when sintered at low temperature of 1000 °C. Nevertheless, as the sintering temperature increased to 1050 °C, the fracture toughness of 0.5 wt% Bi_2O_3-doped HA dropped drastically to 0.66 MPa $m^{1/2}$ and then fluctuated at 0.55–0.61 MPa $m^{1/2}$ when sintered above 1050 °C. Fig. 6 also shows that the addition of 1.0 wt% Bi_2O_3 was detrimental to the fracture toughness of the sintered HA ceramic.

In general, the addition of 0.5 wt% Bi_2O_3-doped HA was found to be most beneficial as the samples exhibited the highest fracture toughness when sintered at temperature of 1000 °C. This observation is significant since Bi_2O_3 could increased the toughness by 40% without causing decomposition of the HA phase. One plausible explanation for the remarkable rise in K_{Ic} in the 0.5 wt% Bi_2O_3-doped HA could be associated with the influence of liquid phase at grain boundary regions that acts to strengthen the grain boundaries of the ceramic, thus creating a torturous path for crack propagation [6,29].

3.5. Microstructure evolution

The SEM images in Fig. 7(c–e) shows the fracture surface of quenched samples (undoped, 0.5 wt% and 1.0 wt% Bi_2O_3-doped HA). It was found that the undoped sample exhibited intergranular fracture mode. This indicates that the grain interior is stronger than the grain boundary. However, the introduction of Bi_2O_3 into HA matrix has altered the fracture mode from intergranular to transgranular. This observation suggested that grain boundary exhibited more resistant to fracture than the grain interior.

A similar grain boundary strengthening effect has been reported in the literature for other Bi_2O_3-doped ceramic system. Olsson and Dunlop [30] and Kanai et al. [31] found an amorphous intergranular Bi-rich phase in the microstructure of Bi_2O_3-doped ZnO varistor. Morris [32] reported that Bi was concentrated within a 2 nm surface layer of ZnO grains as observed with Auger spectroscopy. Yu et al. [25] confirmed that Bi_2O_3 was detected on the grain boundary of Bi_2O_3-doped MnZn ferrite sample.

A comprehensive investigation was carried out by Kobayashi et al. [33]. In their experiment, a high resolution transmission electron microscope (HRTEM) image revealed that both amorphous and Bi-crystalline intergranular phases were present in the grain boundary. The amorphous phase is sandwiched between the Bi-crystalline phases, and theses crystalline phases are in contact with ZnO grains. Based on the observation of Kobayashi et al. [33], it may be the case that such a grain boundary could exist in the current Bi_2O_3-doped HA

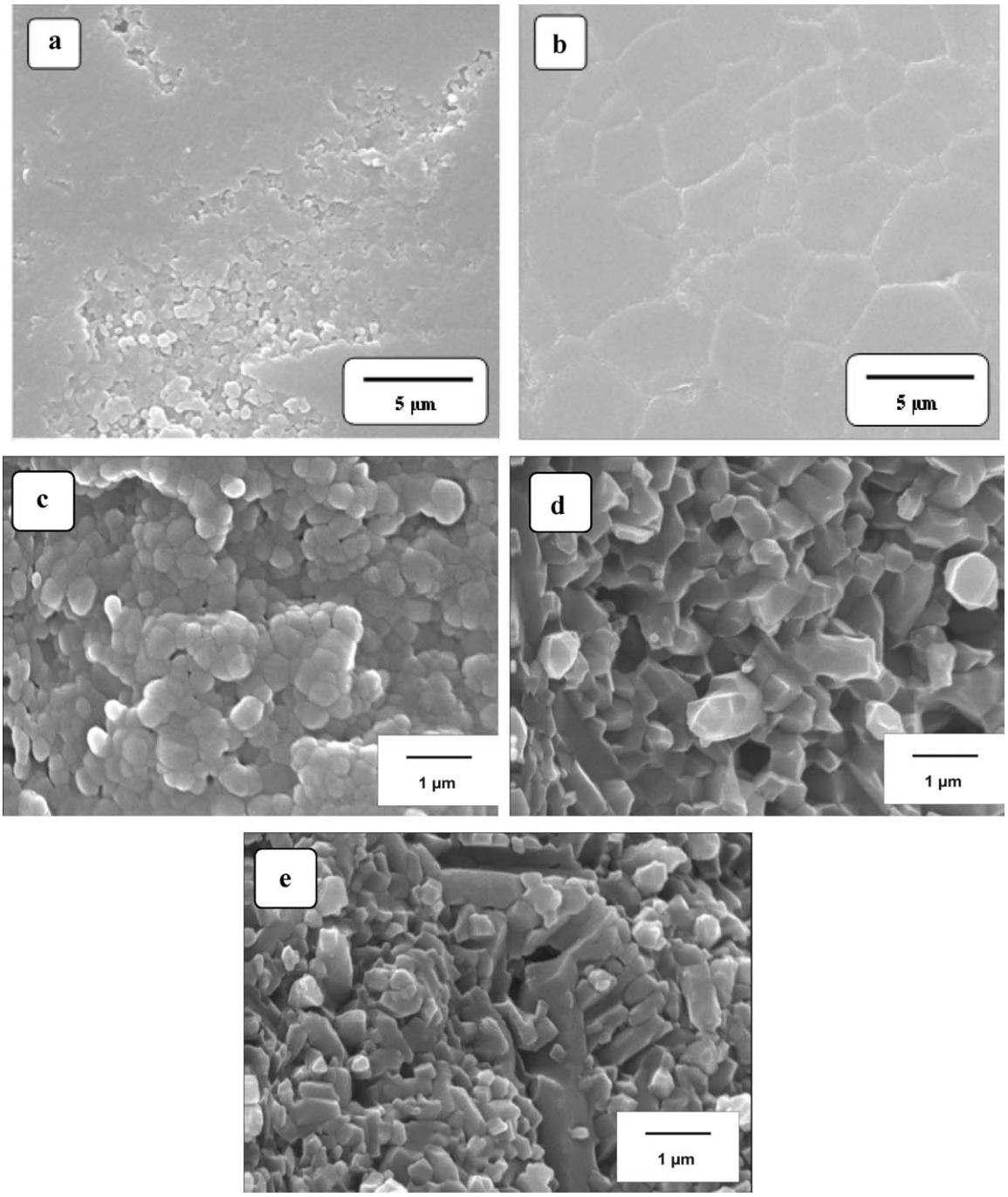

Fig. 7. SEM micrographs of (a) undoped sintered HA at 1000 °C; (b) 0.5 wt% Bi_2O_3-doped HA sintered at 1000 °C and the fracture surface of (c) undoped; (d) 0.5 wt%; (e) 1.0 wt% Bi_2O_3-doped HA, respectively.

system. Eventually, when crack penetrating into the grain boundary, it would require additional energy to break the triple barrier in the grain boundary as compared to normal transgranular fracture.

4. Conclusions

The sinterability of the Bi_2O_3-doped HA compacts was compared in terms of HA phase stability, relative density, Vickers hardness, fracture toughness and Young's modulus. The introduction of Bi_2O_3 was found to have negligible effect on the particle morphology and crystallite size of the HA powder. In terms of phase stability, Bi_2O_3 peak was detected when addition of 0.3 wt% and above of Bi_2O_3 was incorporated into HA powder. XRD analysis of sintered samples revealed that the stability of HA phase was disrupted when addition of 0.3, 0.5 and 1.0 wt% Bi_2O_3 were used and when samples sintered above 1100 °C, 1000 °C and 950 °C, respectively. In general, HA containing 0.5 wt% of Bi_2O_3 was found to be most beneficial in enhancing densification, Young's modulus, hardness and fracture toughness at low temperature of 1000 °C without disrupting the HA phase.

The addition 0.5 wt% Bi-doped HA was able to achieved relative density of >98% as compared to 95.5% for undoped HA when sintered at 1000 °C. For Young's modulus, the highest value of ~103 GPa was recorded for HA samples containing 0.5 wt% Bi_2O_3 when sintered at 1000 °C as compared to 93 GPa for undoped HA when sintered at similar temperature. A maximum hardness of 6.1 GPa and toughness of 1.21 MPa $m^{1/2}$ were also measured at similar composition and sintering temperature.

Acknowledgements

The authors would like to acknowledge the financial support provided by MOSTI under the eScience Fund programme (03-02-03-SF0073).

References

[1] R.N. Correia, M.C.F. Magalhaes, P.A.A.P. Marques, A.M.R. Senos, Wet synthesis and characterization of modified hydroxyapatite powders, J. Mater. Sci.: Mater. Med. 7 (1996) 501–505.
[2] J.-S. Bow, S.-C. Liou, S.-Y. Chen, Structural characterization of room-temperature synthesized nano-sized β-tricalcium phosphate, Biomaterials 25 (16) (2004) 3155–3161.
[3] W. Suchanek, M. Yoshimura, Processing and properties of hydroxyapatite-based biomaterials for use as hard tissue replacement implants, J. Mater. Res. 13 (1998) 94–117.
[4] W. Suchanek, M. Yashima, M. Kakihana, M. Yoshimura, Hydroxyapatite ceramics with selected sintering additives, Biomaterials 18 (1997) 923–933.
[5] G. Muralitharan, S. Ramesh, The effect of MnO_2 addition on the sintering behavior of hydroxyapatite, Biomed. Eng. Appl. Basis Commun. 12 (2000) 43–48.
[6] S.J. Kalita, A. Bhardwaj, H.A. Bhatt, Nanocrytalline calcium phosphate ceramics in biomedical engineering, Mater. Sci. Eng. C 27 (2007) 441–449.
[7] M.A. Fanovich, J.M.P. Lopez, Influence of temperature and additives on the microstructure and sintering behaviour of hydroxyapatites with different Ca/P ratios, J. Mater. Sci.: Mater. Med. 9 (1998) 53–60.
[8] S. Ramesh, C.Y. Tan, C.L. Peralta, W.D. Teng, The effect of manganese oxide on the sinterability of hydroxyapatite, Sci. Technol. Adv. Mater. 8 (2007) 257–263.
[9] N. Yang, H. Sun, Biocoordination chemistry of bismuth: recent advances, Coord. Chem. Rev. 251 (2007) 2354–2366.
[10] T.J. Webster, E.A. Massa-Schlueter, J.L. Smith, E.B. Slamovich, Osteoblast response to hydroxyapatite doped with divalent and trivalent cations, Biomaterials 25 (2004) 2111–2121.
[11] S. Ramesh, C.Y. Tan, I. Sopyan, M. Hamdi, W.D. Teng, Consolidation of nanocrystalline hydroxyapatite powder, Sci. Technol. Adv. Mater. 8 (2007) 124–130.
[12] ASTM E1876-97, Standard test method for dynamic Young's modulus, shear modulus and Poisson's ratio by impulse excitation of vibration, Annual Book of ASTM Standards (1998).
[13] K. Niihara, Indentation microfracture of ceramics—its application and problems, Ceram. Jpn. 20 (1985) 12–18.
[14] M. Peiteado, M.A. de, L.A. Rubia, M.J. Velasco, F.J. Valle, A.C. Caballero, Bi_2O_3 vaporization from ZnO-based varistors, J. Eur. Ceram. Soc. 25 (2005) 1675–1680.
[15] Y.-M. Chiang, W.D. Kingery, L.M. Levinson, Compositional changes adjacent to grain boundaries during electrical degradation of a ZnO varistor, J. Appl. Phys. 53 (1982) 1765–1768.
[16] R. Metz, H. Delalu, J.R. Vignalou, N. Achard, M. Elkhatib, Electrical properties of varistors in relation to their true bismuth composition after sintering, Mater. Chem. Phys. 63 (2000) 157–162.
[17] B.D. Culity, S.R. Stock, Elements of X-ray Diffraction, 3rd ed., Prentice-Hall Inc., 2001, pp. 167–170.
[18] H.S. Liu, T.S. Chin, L.S. Lai, S.Y. Chiu, K.H. Chung, C.S. Chang, M.T. Lui, Hydroxyaptite synthesized by a simplified hydrothermal method, Ceram. Int. 23 (1997) 19–25.
[19] C.K. Wang, C.P. Ju, J.H. Chern-Lin, Effect of doped bioactive glass on structure and properties of sintered hydroxyapatite, Mater. Chem. Phys. 53 (1998) 138–149.
[20] P.E. Wang, T.K. Chaki, Sintering behaviour and mechanical properties of hydroxyapatite and dicalcium phosphate, J. Mater. Sci.: Mater. Med. 4 (1993) 150–158.
[21] S. Raynaud, E. Champion, D. Bernache-Assollant, Calcium phosphate apatites with variable Ca/P atomic ratio. II. Calcination and sintering, Biomaterials 23 (2002) 1073–1080.
[22] J.D. Santos, P.L. Silva, J.C. Knowles, G.W. Hasting, Liquid phase sintering of hydroxyapatite by phosphate and silicate glass additions: structure and properties of the composites, J. Mater. Sci: Mater. Med. 6 (1995) 348–352.
[23] A. Bandyopadhyay, E.A. Withey, J. Moore, S. Bose, Influence of ZnO doping in calcium phosphate ceramics, Mater. Sci. Eng. C 27 (2007) 14–17.
[24] V. Gil, J. Tartaj, C. Moure, P. Duran, Rapid densification by using Bi_2O_3 as an aid for sintering of gadolinia-doped ceria ceramics, Ceram. Int. 33 (2007) 471–475.
[25] Z. Yu, K. Sun, L. Li, Y. Liu, Z. Lan, H. Zhang, Influences of Bi_2O_3 on microstructure and magnetic properties of MnZn ferrite, J. Magn. Magn. Mater. 320 (2008) 919–923.
[26] M. Hirano, T. Oda, K. Ukai, Y. Mizutani, Effect of Bi_2O_3 additives in Sc stabilized zirconia electrolyte on a stability of crystal phase and electrolyte properties, Solid State Ion. 158 (2003) 215–223.
[27] S.J. Kalita, S. Bose, H.L. Hosick, A. Bandyopadhyay, $CaO–P_2O_5–Na_2O$ based sintering additives for hydroxyapatite (HAp) ceramics, Biomaterials 25 (2004) 2331–2339.
[28] F.P. Filho, R.E.F.Q. Nogueira, M.P.F. Graca, M.A. Valente, A.S.B. Sombra, C.C. Silva, Structural and mechanical study of the sintering effect in hydroxyapatite doped with iron oxide, Phys. B: Condens. Matter 403 (2008) 3826–3829.
[29] G. Georgiou, J.C. Knowles, Glass reinforced hydroxyapatite for hard tissue surgery. Part 1. Mechanical properties, Biomaterials 22 (2001) 2811–2815.
[30] E. Olsson, D.L. Dunlop, Characterization of individual barriers in a ZnO varistor material, J. Appl. Phys. 66 (1989) 3666–3675.
[31] H. Kanai, M. Imai, T. Takahashi, A high-resolution transmission electron microscope study of a zinc oxide varistor, J. Mater. Sci. 20 (1985) 3957–3966.
[32] W.G. Morris, Physical properties of the electrical barriers in varistors, J. Vac. Sci. Technol. 13 (1976) 926–931.
[33] K.-I. Kobayashi, O. Wada, M. Kobayashi, Y. Takada, Continuous existence of bismuth at grain boundaries of zinc oxide varistor without intergranular phase, J. Am. Ceram. Soc. 81 (1998) 2071–2076.